

Developing a Compositional Reservoir Model for Investigating the Effect of Interfacial Tension on Oil Recovery

Shahrabadi, Abbas^{*+}; Dabir, Bahram; Sadi, Maryam

Department of Chemical Engineering, Amirkabir University of Technology, Tehran, I.R. IRAN

ABSTRACT: *In this paper, a simplified formulation for compositional reservoir simulator is presented. These types of simulators are used when inter-phase mass transfer depends on phase composition as well as pressure. The procedure for solving compositional model equations is completely described. For equilibrium calculation, property estimation Peng Robinson equation of state is used. This equation was tuned using some data from swelling test and saturation pressure data. It is another purpose of this work, to show how the gas oil interfacial tension impresses the predictions of developed compositional model. Application of the simulator to simulate the results of oil recovery from displacement tests is presented. A good agreement was achieved between the experimental data and model predictions.*

KEY WORDS: *Interfacial tension, Simulator, Compositional model, Enhanced oil recovery.*

INTRODUCTION

Compositional reservoir simulators are important tools for predicting the performance of oil recovery methods when oil and gas undergo vigorous mass transfer during the recovery process. These processes include nitrogen injection into a gas condensate or volatile oil reservoir during the primary production period, CO₂ or enriched gas injection during the enhanced oil recovery from oil reservoirs. The design of these processes requires an accurate prediction of the vapor liquid equilibrium between oil and gas. Generally, vapor liquid equilibrium is done using an equation of state. Recently cubic equation of state such as *Peng Robinson* and *Soave Redlich Kwong* appear to be more popular for the

correlation of fluid properties. The first compositional reservoir model that utilize an equation of state for phase equilibrium are described by *Fussel* and *Fussel* [1]. In their formulation, the simultaneous solution of $n_b(n_c+1)$ non-linear equations are required, where n_b is the grid block number and n_c is the number of components. *Coats* [2] presented a fully implicit compositional model based on *Newton* iteration, to simulate compositional reservoir problems with an equation of state. His formulation requires the simultaneous solution of $n_b(2n_c+4)$ equations. The stability of *Coats* model is better than *Fussel* and *Fussel* model, but the computational cost of his model may become prohibitive for systems

** To whom correspondence should be addressed.*

+E-mail: ashahrabadi@aut.ac.ir

1021-9986/06/4/77

8/\$/2.80

containing a large number of grid blocks and components. *Watts* [3] presented the sequential implicit method to solve the compositional flow difference equations. An attempt was made to combine the advantages of IMPECS (Implicit in pressure explicit in composition and saturation) while retaining some of stability characteristics of the implicit method. *Quandalle* and *Savary* [4] presented a method, implicit in pressure and saturation and explicit in composition. Recently, compositional stream line simulators for assessment of miscible/near miscible gas injection process performance are widely used.

These simulators have significant potential to accommodate requirement for accurate and reliable production forecasts. These requirements include high resolution descriptions of permeability heterogeneity and appropriate representation of the phase behavior including a sufficient number of components in the equation of state representation of reservoir fluid [5]. Numerous authors have contributed to the development of stream line simulator [6-10].

In the area of compositional simulation variation in gas oil relative permeability as a function of Interfacial Tension (IFT) is of particular importance. Many standard compositional simulators utilize a model, first proposed by *Coats* [2] which employs simple linear interpolation to modify the relative permeability curves at different values of IFT. The interpolated relative permeabilities take the form:

$$k_r = r^n k_{rb} + (1 - r^n) k_{rm} \quad (1)$$

Where $r = \sigma/\sigma^*$, σ is the gas oil IFT under consideration, σ^* the base gas oil IFT, n read-in exponent, k_{rb} the phase relative permeability measured at σ^* and k_{rm} the miscible displacement phase relative permeability (generally taken to be a linear function of saturation). In this paper, a sequential formulation for compositional reservoir simulator and solution method for compositional equations are presented. Basically, it uses the ideas of *Nghiem et al.* [11], but in this formulation the implicit transmissibilities have been used. In this work for calculating the gas oil IFT Macleod-Sugden correlation [12] was used.

COMPOSITIONAL MODEL EQUATION

The starting point for the compositional formulation is

the molar continuity equation for any component i and water:

$$\frac{\partial N_i}{\partial t} = \theta_i, \quad i = 1, 2, \dots, n_c \quad (2)$$

$$\frac{\partial N_{n_c+1}}{\partial t} = \theta_{n_c+1} \quad (3)$$

N_i denotes the moles of component i per unit of reservoir volume and N_{n_c+1} is the moles of water per unit of reservoir volume and are related to the phase molar densities, saturations and composition as follows:

$$N_i = \phi (\xi_o S_o x_i + \xi_g S_g y_i) \quad (4)$$

$$N_{n_c+1} = \phi \xi_w S_w \quad (5)$$

$\theta_i (\theta_{n_c+1})$ which is the rate of accumulation of component i (water) is equal to the divergence of the flux of component i plus rate of injection or production. Thus:

$$\theta_i = \nabla \cdot \left[\xi_o x_i \frac{kk_{ro}}{\mu_o} \nabla \Phi + \xi_g y_i \frac{kk_{rg}}{\mu_g} \nabla \Phi_g \right] + q_i \quad (6)$$

$$\theta_{n_c+1} = \nabla \cdot \left[\xi_w \frac{kk_{rw}}{\mu_w} \nabla \Phi_w \right] + q_w \quad (7)$$

In the above equations:

$$\nabla \Phi_o = \nabla P_o - \gamma_o \nabla h \quad (8)$$

$$\nabla \Phi_g = \nabla P_o + \nabla P_{cog} - \gamma_g \nabla h \quad (9)$$

$$\nabla \Phi_w = \nabla P_o - \nabla P_{cow} - \gamma_w \nabla h \quad (10)$$

$$\gamma_j = C_1 \frac{g}{g_c} \rho_j, \quad j = o, g, w \quad (11)$$

The molar continuity equation for the hydrocarbon system is obtained by summing eq. (2) over N_c hydrocarbon:

$$\frac{\partial N}{\partial t} = \theta \quad (12)$$

In this equation:

$$N = \phi (\xi_o S_o + \xi_g S_g) \quad (13)$$

$$\theta_i = \nabla \cdot \left[\xi_o \frac{kk_{ro}}{\mu_o} \nabla \Phi_o + \xi_g \frac{kk_{rg}}{\mu_g} \nabla \Phi_g \right] + q_t \quad (14)$$

$$q_t = \sum_{i=1}^{n_c} q_i \quad (15)$$

Multiplying equations (2), (3) and (12) by grid block volume (V_b) and writing those equations in finite difference form:

$$\frac{V_b}{\Delta t} (N_i^{n+1} - N_i^n) = \Delta(T_o^{n+1} x_i^{n+1} (\Delta P_o^{n+1} - \gamma_o^n \Delta h)) + \Delta(T_g^{n+1} y_i^{n+1} (\Delta P_o^{n+1} + \Delta P_{cog}^n - \gamma_o^n \Delta h)) + q_i V_b \quad (16)$$

$$\frac{V_b}{\Delta t} (N_w^{n+1} - N_w^n) = \Delta T_w^{n+1} (\Delta P_o^{n+1} - \Delta P_{cow}^n - \gamma_w^n \Delta h) + q_w V_b \quad (17)$$

$$\frac{V_b}{\Delta t} (N^{n+1} - N^n) = \Delta(T_o^{n+1} (\Delta P_o^{n+1} - \gamma_o^n \Delta h)) + \Delta(T_g^{n+1} (\Delta P_o^{n+1} + \Delta P_{cog}^n - \gamma_o^n \Delta h)) + q_t V_b \quad (18)$$

In the above equations :

$$T_j = C_2 \frac{k k_{ij} A}{\mu_j \Delta L_t}, \quad j = o, g, w \quad (19)$$

It is assumed at the end of each time step the gas and oil are in phase equilibrium. It means that the interphase thermodynamic exchange in the reservoir is rapid compared with fluid flow. The condition for thermodynamic equilibrium is established by the equality of the oil and gas phase chemical potentials, or fugacity for each component:

$$f_i^o(T, P, x_i) = f_i^g(T, P, y_i) \quad (20)$$

From a material balance on the oil and gas phases, the following equation is obtained:

$$F z_i = L x_i + V y_i, \quad i = 1, 2, \dots, n_c \quad (21)$$

The following equations are used in solution of eq. (20):

$$\sum_{i=1}^{n_c} x_i - 1 = 0 \quad (22)$$

$$\sum_{i=1}^{n_c} y_i - 1 = 0 \quad (23)$$

$$\sum_{i=1}^{n_c} \frac{z_i (K_i - 1)}{1 + V(K_i - 1)} = 0 \quad (24)$$

The definition of saturation gives the constraint equation:

$$S_o + S_g + S_w = 1 \quad (25)$$

Each grid block has its own set of above equations. The basic idea used in this work is to reduce the unknowns into one unknown for each grid block in terms of grid block pressure.

CONSTRUCTION OF PRESSURE EQUATION

Adding equations (17) and (18) results in the pressure equation:

$$\frac{V_b}{\Delta t} [(N + N_w)^{n+1} - (N + N_w)^n] = \Delta(T_o^{n+1} (\Delta P_o^{n+1} - \gamma_o^n \Delta h)) + \Delta(T_g^{n+1} (\Delta P_o^{n+1} + \Delta P_{cog}^n - \gamma_g^n \Delta h)) + \Delta(T_w^{n+1} (\Delta P_o^{n+1} + \Delta P_{cog}^n - \gamma_w^n \Delta h)) + V_b (q_t + q_w) \quad (26)$$

The following approximations apply to the flow terms:

$$T_j^{n+1} = T_j^l, \quad j = o, g, w \quad (27)$$

$$x_i^{n+1} = x_i^l \quad (28)$$

$$y_i^{n+1} = y_i^l \quad (29)$$

l denotes the last iteration. The pressure equation is solved using the iterative biconjugate gradient method for sparse matrices[13].

COMPOSITION AND SATURATION EQUATIONS

Composition of each component is calculated at each iteration using pressure of the same iteration. First the number of moles of component i is calculated from eq. (16) and then total moles from eq. (18). z_i is obtained by the ratio of N_i to N:

$$N_i^{l+1} = \frac{\Delta t}{V_b} [\Delta(T_o^{n+1} x_i^{n+1} (\Delta P_o^{n+1} - \gamma_o^n \Delta h)) + \Delta(T_g^{n+1} y_i^{n+1} (\Delta P_o^{n+1} + \Delta P_{cog}^n - \gamma_g^n \Delta h)) + q_i V_b] + N_i^n \quad (30a)$$

$$N^{l+1} = \frac{\Delta t}{V_b} [\Delta(T_o^{n+1} (\Delta P_o^{n+1} - \gamma_o^n \Delta h)) + \Delta(T_g^{n+1} (\Delta P_o^{n+1} + \Delta P_{cog}^n - \gamma_g^n \Delta h)) + \Delta(T_w^{n+1} (\Delta P_o^{n+1} + \Delta P_{cog}^n - \gamma_w^n \Delta h)) + q_t V_b] + N^n \quad (30b)$$

$$z_i^{l+1} = \frac{N_i^{l+1}}{N^{l+1}} \quad (30c)$$

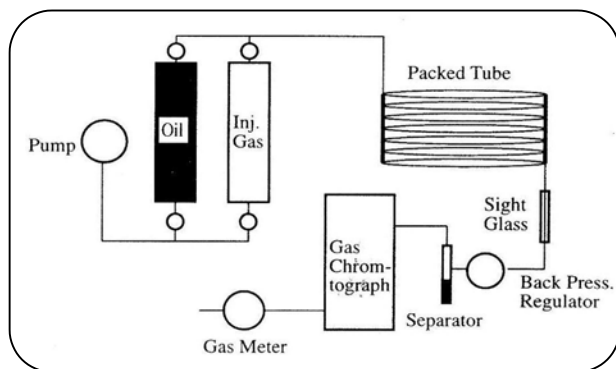


Fig. 1: The schematic apparatus of slim tube.

Water saturation is obtained from eq. (17):

$$N_w^{l+1} = \frac{\Delta t}{V_b} \left[\Delta T_w^{n+1} (\Delta P_o^{n+1} - \Delta P_{cow}^n - \gamma_w^n \Delta h) + q_w V_b \right] + N_w^n \quad (31a)$$

$$S_w^{l+1} = \frac{N_w^{l+1}}{(\phi \xi_o)^{l+1}} \quad (31b)$$

After calculating compositions, flash calculation is performed on calculated compositions in each grid block at block pressure and temperature for obtaining amount of liquid and vapor (L, V). Then gas and oil saturation is calculated from this equation:

$$S_g^{l+1} = \frac{V \xi_o^{l+1} (1 - S_w^{l+1})}{\xi_g^{l+1} + V (\xi_o + \xi_g)^{l+1}} \quad (32a)$$

$$S_o^{l+1} = 1 - S_g^{l+1} - S_w^{l+1} \quad (32b)$$

Where:

$$V = \frac{\xi_g S_g}{\xi_o S_o + \xi_g S_g} \quad (33)$$

SOLUTION PROCEDURE

To solve the above set of equations over a time step the following procedure is used:

1-Solving pressure equation (eq. 26) using the iterative biconjugate gradient method for sparse matrix.

2-Obtaining water saturation (eq. 31) and composition of each component (Eq. 30) at each grid block using the block pressures computed in step 1.

3- Performing flash calculation on calculated composition in step 2 at block temperature and pressure

Table 1: Specification of slim tube.

Initial Diameter (mm)	4.65
Length (m)	12.78
Pore Volume (cm ³)	94.73
Porosity (%)	43.7
Permeability (Darcy)	4.850
Porous Media	Glass beads

in each grid block in order to obtain L and V.

4- Calculating oil and gas saturations. (eq. 33)

5- Updating T_j , x_i , y_i , N and N_w .

The above steps are repeated until convergence is achieved.

EXPERIMENTAL STUDIES

The recovery curves obtained in this study were determined using the slim tube apparatus. Basically it consisted of an injection cell, slim tube, sight glass and backpressure regulator. The schematic of experimental apparatus is shown in Fig. 1. The specifications of slim tube is given in table 1. For each displacement test, the tube was saturated initially with reservoir oil sample. The oil sample used in this work was selected from an Iranian oil reservoir. Also a gas sample from a gas reservoir of Iran was used as displacing agent. Compositional analyses of oil and gas and characterization of plus fraction are given in tables 2 and 3. Bubble point pressure and swelling data are also included. In each step of the test, the oil was displaced by injecting gas into the tube at a constant injection rate of 15 cm³/hr and outlet pressure was kept constant by back pressure regulator. In each displacement test, about 1.2 pore volume of gas was injected through the slim tube. During different run the amount of produced oil and gas should be measured. Referring to the measured volumes of the produced oil and gas, recovery factor could be calculated.

RESULTS AND DISCUSSION

This study was performed to show the effect of including interfacial tension in relative permeability curves on simulation results of slim tube experiment. Five displacement tests at different pressures were carried out and the oil recoveries as a function of

Table 2: Compositional analysis of oil, gas sample and swelling and saturation data.

Component	Reservoir Fluid	Injection Gas	Recombined Reservoir Fluid + Gas					
H ₂ S	0.0012	0.0047	0.001528	0.001873	0.002153	0.002383	0.002571	0.002732
N ₂	0.0004	0.0414	0.004233	0.008267	0.011532	0.014214	0.016411	0.01829
CO ₂	0.0125	0.0217	0.013357	0.01426	0.014991	0.015592	0.016084	0.016505
C ₁	0.2530	0.8490	0.308699	0.367335	0.414793	0.453791	0.485726	0.513042
C ₂	0.0570	0.0516	0.056494	0.055967	0.055541	0.05519	0.054903	0.054658
C ₃	0.0471	0.0174	0.044314	0.041388	0.039019	0.037073	0.035479	0.034116
IC ₄ +NC ₄	0.0440	0.0086	0.040683	0.037198	0.034377	0.032059	0.030161	0.028538
IC ₅ +NC ₅	0.0217	0.0030	0.019949	0.018108	0.016619	0.015394	0.014392	0.013535
C ₆	0.0398	0.0013	0.036201	0.032417	0.029355	0.026839	0.024778	0.023016
C ₇	0.0351	0.0010	0.031911	0.02856	0.025847	0.023618	0.021793	0.020232
C ₈	0.0330	0.0003	0.029941	0.026725	0.024122	0.021983	0.020232	0.018734
C ₉₊	0.4553	0.0000	0.41269	0.367901	0.331651	0.301862	0.277469	0.256604
Solution GOR, M ³ /M ³ (Scf/STB)	82 (459.2)	-	94 (529.7)	111 (621.5)	127 (714.0)	144 (806.6)	160 (897.2)	176 (988.4)
Bubble Point Pressure kPa (psia)	11,925 (1730)		14,592 (2117)	17,866 (2592)	21,719 (3151)	24,091 (3495)	26,413 (3832)	29,171 (4232)
Calculated Data								
Bubble Point Pressure kPa (psia)	11,911 (1728)		14,685 (2130.5)	18,021 (2614.5)	21,126 (3064.9)	24,031 (3486.4)	26,715 (3875.7)	29,287 (4248.9)
Swelling factor	1.00		1.03	1.07	1.11	1.14	1.18	1.21

Table 3: Characterization of C₉⁺.

Molecular Weight	194
Specific Gravity	0.8897

injected pore volume were measured. The influence of interfacial tension on the results of developed model was examined in two runs with different relative permeability curves. The model was run once with fixed relative permeability curves (Immiscible condition), while in the next run the variable relative permeability curves as a function of both saturation and interfacial tension was used (Miscible condition). For oil and gas system, relative permeabilities as functions of saturation only are represented as \bar{k}_{rg} , \bar{k}_{ro} . To include interfacial tension (σ) in relative permeabilities, the following equations were used:

$$k_{ro} = \left(1 - e^{-a_o r}\right) \bar{k}_{ro} + e^{-a_o r} S_o \quad (34)$$

$$k_{rg} = \left(1 - e^{-a_g r}\right) \bar{k}_{rg} + e^{-a_g r} S_g \quad (35)$$

In the above equations a_g , a_o are positive numbers and are used as adjustable parameters. Interfacial tension between vapor and liquid phases at 20,678 kPa (3000 psia) and 83°C (181°F) at equilibrium is considered as σ^* .

A one dimensional compositional model composed of 30 grid blocks was employed to simulate the slim tube experiments. The predicted oil recovery vs. injected gas volume for the two simulated runs (different relative permeability curves) are compared against experimental data in Figs. 2-6. Comparisons show that use of fixed relative permeability curves underestimates the oil recoveries while including interfacial tension in relative permeabilities improves the predictions.

Now, we define a new parameter as the difference between ultimate recovery obtained by fixed relative permeability curve and relative permeability including IFT. We call this parameter as DR. Fig. 7 shows DR

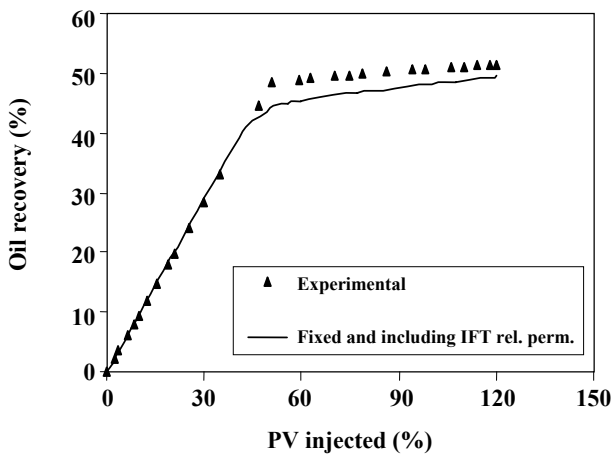


Fig. 2: Oil recovery curve vs. PV injected at pressure 13,786 kPa (2000 psia).

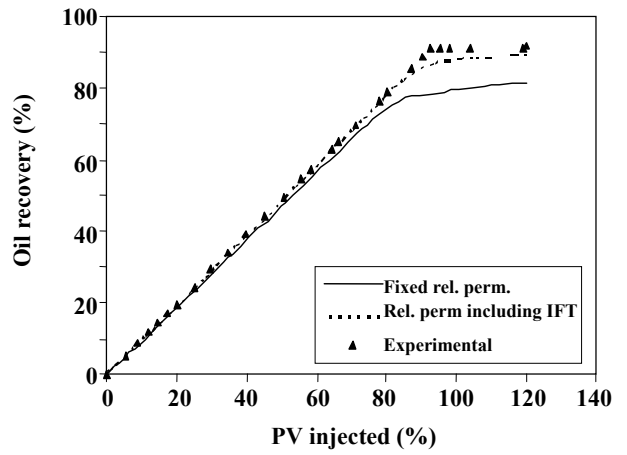


Fig. 5: Oil recovery curve vs. PV injected at pressure 41,357 kPa (6000 psia).

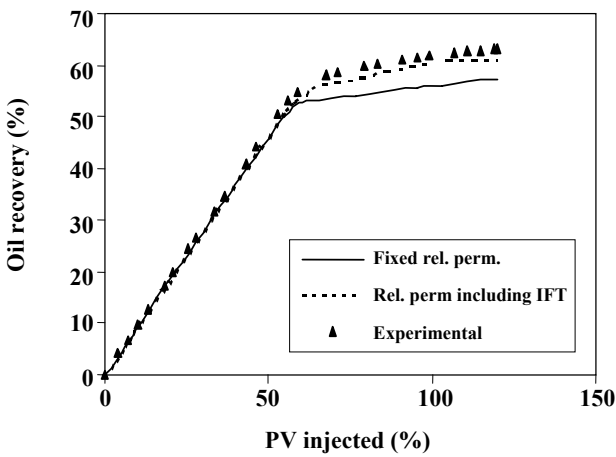


Fig. 3: Oil recovery curve vs. PV injected at pressure 20,678 kPa (3000 psia).

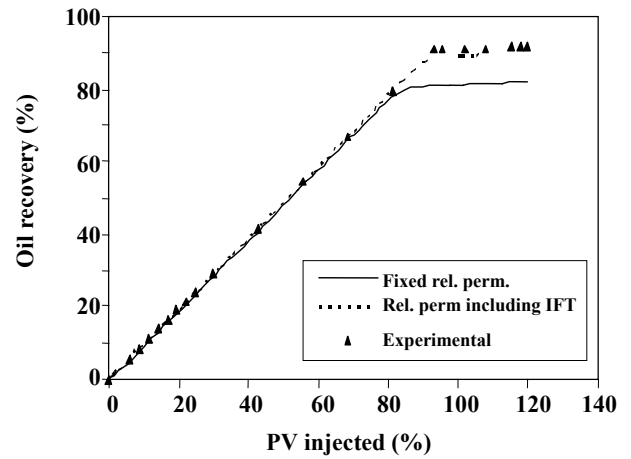


Fig. 6: Oil recovery curve vs. PV injected at pressure 44,804 kPa (6500 psia).

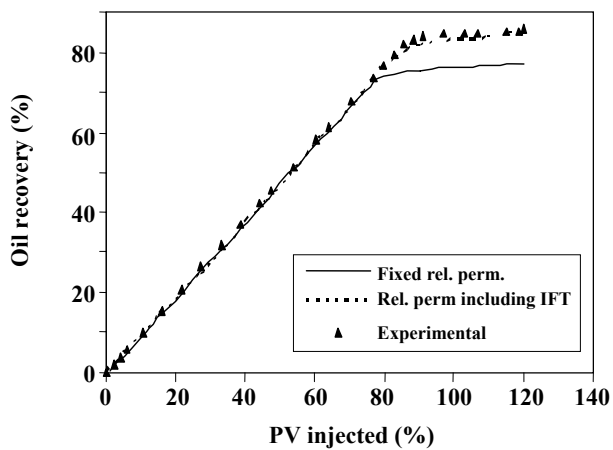


Fig. 4: Oil recovery curve vs. PV injected at pressure 34,464 kPa (5000 psia).

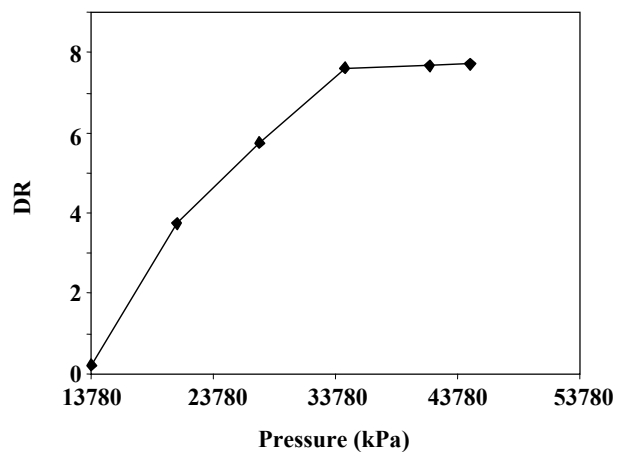


Fig. 7: Difference in oil recovery between fixed and IFT dependent relative permeability curve in different pressures.

at different pressure. The difference between ultimate oil recoveries obtained using fixed relative permeability and IFT included in curves is small at low pressure but the difference is intensified at high pressures. This is due to the fact that low pressure corresponds to the immiscible zone and IFT has low effect on recovery results. Therefore at low pressures including IFT in relative permeability curves can not improve the predictions, but as pressure increases it can match the predictions to the experimental results in a closer margin. In other words, high pressure corresponds to the miscible zone and IFT plays a key role in oil recovery at high pressure. Therefore, including IFT in relative permeability curve improves the results of model drastically at high pressure

CONCLUSIONS

Based on the materials presented in this study, the following conclusions are obtained:

1- The procedure to formulate a three phase compositional reservoir model was presented.

2- A method for solving compositional model equations was described.

3- An experimental setup using slim tube was prepared. This was used in few displacement tests. During each test oil recoveries at different injected gas volumes were measured.

4-The model predictions were compared against measured laboratory recovery values which showed a good agreement between them.

5- The effect of including IFT in relative permeability curves on the outputs from model was studied.

6-Comparison between model outputs with and without including IFT in relative permeability curves indicated that at low pressures, including the IFT in relative permeability curves has no effect (rather a minor effect) on model results, while at high pressures this effect is considerable.

7- A new parameter was defined as difference between ultimate recovery of cases where IFT was included in relative permeability curve and the case, with fixed relative permeability curve. From plot of this parameter, which was called DR, versus pressure it can be easily inferred that as pressure increases this parameter also increases until a point on the pressure axis is reached where the curve start to level off. This pressure can be considered as Minimum Miscibility Pressure.

Nomenclature

A	Area perpendicular to flow (m^2)
C_1	Conversion factor in equation (11)
C_2	Conversion factor in equation (19)
F	Feed
f_i^j	Fugacity of component i in phase j (atm)
g	Gravitational acceleration (m/s^2)
h	Depth (m)
k	Absolute permeability (mdarcy)
k_{ij}	Relative permeability of phase j (immiscible condition)
\bar{k}_{rj}	Relative permeability of phase j (miscible condition)
K_i	K-value of component i
L	Ratio of moles in liquid phase to the total number of moles in the mixture
L_t	Length (m)
N	Moles of total hydrocarbon per unit of reservoir volume ($mole/m^3$)
N_i	Moles of component i per unit of reservoir volume ($mole/m^3$)
N_{n_c+1}	Moles of water per unit of reservoir volume ($mole/m^3$)
P	Pressure of mixture at equilibrium (kPa)
P_j	Pressure of phase j (kPa)
P_{cog}	Oil / gas capillary pressure (psia)
P_{cow}	Water / oil capillary pressure (psia)
q_i	Molar injection / production rate of component i per unit volume ($mole/m^3.s$)
q_t	Molar injection / production rate of hydrocarbon per unit volume ($mole/m^3.s$)
q_w	Molar injection / production rate of water per unit volume ($mole/m^3.s$)
r	Ratio of IFT to base IFT
S_j	Saturation of phase j
t	Time (s)
T	Temperature ($^{\circ}R$)
T_j	Transmissibility of phase j ($mole/kPas$)
V	Ratio of moles in vapor phase to the total number of moles in the mixture
V_b	Block volume (m^3)
x_i	Mole fraction of component i in oil phase
y_i	Mole fraction of component i in gas phase
z_i	Mole fraction of component i in hydrocarbon

Greek Symbols

θ_i	The rate of accumulation of component i (mole/m ³ .s)
θ_{n_c+1}	The rate of accumulation of water (mole/m ³ .s)
θ	The rate of accumulation of total hydrocarbon (mole/m ³ .s)
ϕ	Porosity
γ_j	Specific weight of phase j (N/m ³)
μ_j	Viscosity of phase j (kg/m.s)
ρ_j	Mass density of phase j (kg/m ³)
ξ_j	Molar density of phase j (mole/m ³)
Δ	Difference operator
∇	Gradient operator
$\nabla \cdot$	Divergence operator
Φ_j	Potential of phase j (kPa)
σ	Interfacial tension (dyne/cm)
σ^*	Base interfacial tension (dyne/cm)

Received : 17th September 2005 ; Accepted : 1st May 2006

REFERENCES

- [1] Fussell, L.T. and Fussell, D.D., An Iterative Technique for Compositional Reservoir Models, *Society of Petroleum Engineering Journal*, 211 (Aug. 1979).
- [2] Coats, K.H., An Equation of State Compositional Model, *Society of Petroleum Engineering Journal*, 363 (Oct. 1980).
- [3] Watts, J.W., Reservoir Simulation: Past, Present, and Future, Paper SPE 38441, Proceedings of the 14th SPE Symposium on Reservoir Simulation, Dallas, TX, June 8-11 (1997).
- [4] Quandalle, P. and Savary, D., An Implicit in Pressure and Saturations Approach to Fully Compositional Simulation, Paper SPE 18423 Presented at the Symposium on Reservoir Simulation, Houston, TX Feb. 6-8 (1989).
- [5] Jessen, K., Orr, Jr., F.M., Gravity Segregation and Compositional Reservoir Simulation, SPE 89448 Presented at the SPE/DOE Fourteenth Symposium on Improved Oil Recovery, Tulsa, Oklahoma, (2004).
- [6] Datta-Gupta, A. and KING, M.J., A Semi Analytical Approach to Tracer Flow Modeling in Heterogeneous Permeable Media, *Advances in Water Resources*, **18**, 9 (1995).
- [7] Thiele, M.R., Batycky, R.P., Blunt, M.J. and Orr, Jr., F.M., Simulating Flow in Heterogeneous Media Using Streamtubes and Streamlines, *SPE Reservoir Engineering*, **10** (1), 5 (1996).
- [8] Crane, M., Bratvedt, F., Bradvedt, K. and Olufsen, R., A Fully Compositional Streamline Simulator, SPE 63156 Presented at the SPE Annual Technical Conference and Exhibition, Dallas, TX, (2000).
- [9] Ichiro, O., Datta-Gupta, A. and King, M.J., Time Step Selection During Streamline Simulation Via Transverse Flux Correction, SPE 79688 Presented at the SPE Reservoir Simulation Symposium, Houston, TX, (2003).
- [10] Seto, C.J., Jessen, K. and Orr Jr., F.M., Compositional Streamline Simulation of Field Scale Condensate Vaporization by Gas Injection, SPE 79690 Presented at the SPE Reservoir Simulation Symposium, Houston, TX, (2003).
- [11] Nghiem, L.X., Fong, D.K. and Aziz, K., Compositional Modeling with an Equation of State, *Society of Petroleum Engineering Journal*, 687 (Dec. 1981).
- [12] Reid, R.C., Prausnitz, J.M. and Sherwood, T.K., "The Properties of Gases and Liquids", Third Edition, McGraw Hill Inc., New York City (1977).
- [13] Press, W.H., Teukolsky, S.A., Vetterling, W.T. and Flannery, B.P., Numerical Recipes in Fortran 77, Cambridge University Press (1992).